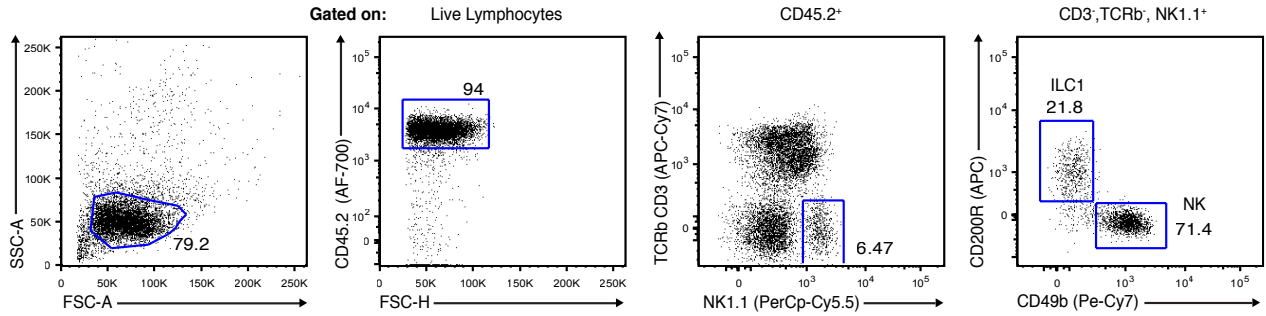
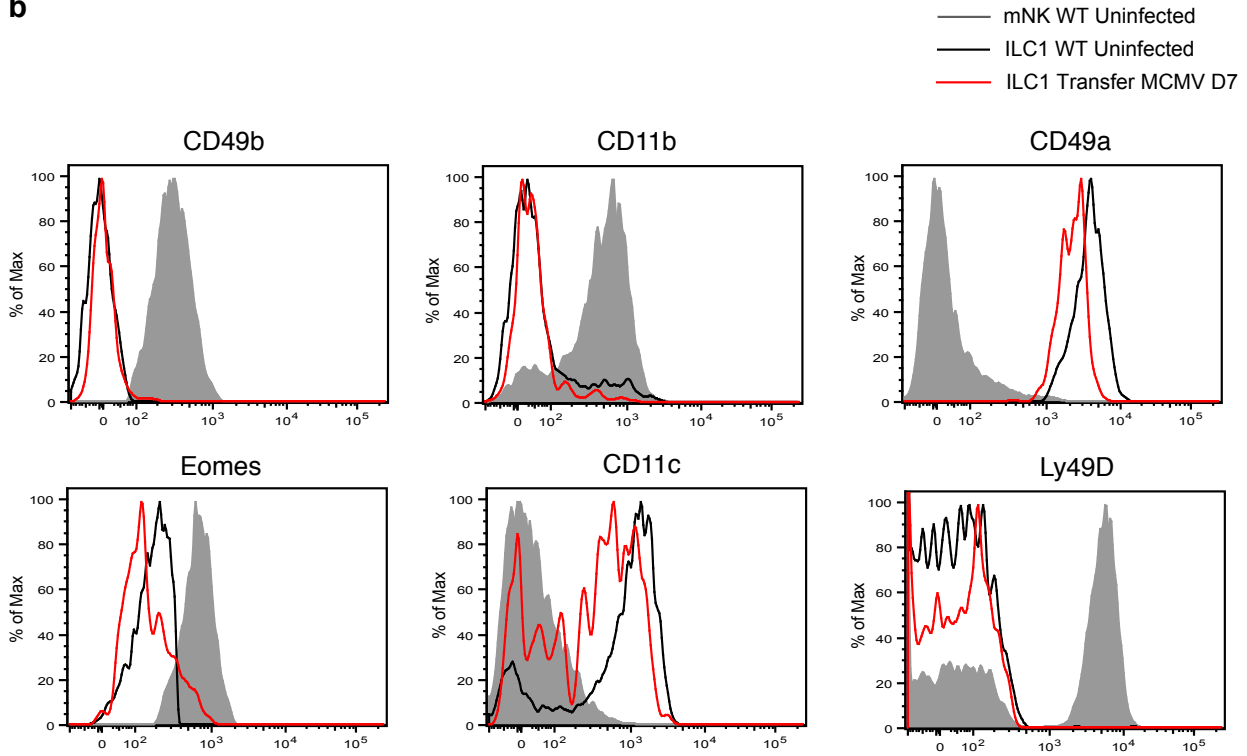


Supplementary Figure 1

a



b

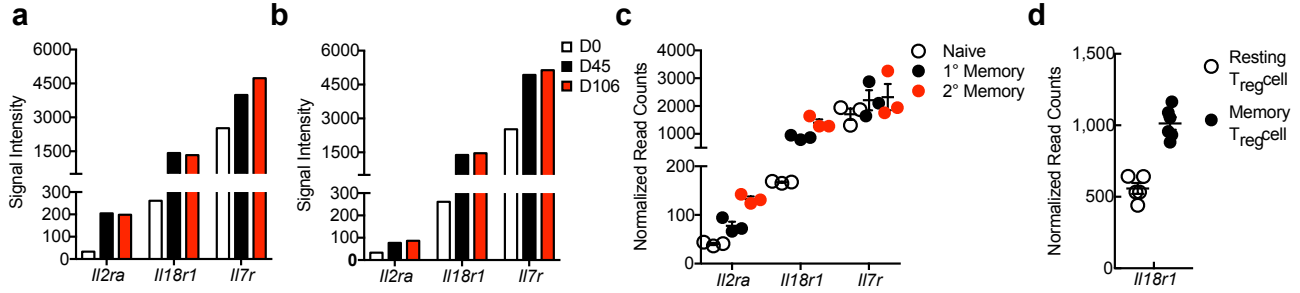


Supplementary Figure 1

Figure S1. Related to Figure 2. Phenotypic and functional stability of Liver ILC1 during MCMV challenge.

(a) Flow cytometry gating strategy for identifying Liver ILC1. **(b)** 4×10^4 liver ILC1 ($\text{Lin}^-\text{NK1.1}^+\text{CD49b}^-\text{CD200r1}^+\text{CD11b}^-\text{Ly49H}^-$) were sort purified from CD45.1^+ mice, adoptively transferred i.v. into Ly49H -deficient CD45.2^+ WT hosts, and subsequently infected with MCMV. Histograms show indicated cell surface markers on liver ILC1 and mNK cells from uninfected WT mice and adoptively transferred liver ILC1 recovered 7 days PI. Data are representative of 3 independent experiments with $n=3$ mice per group.

Supplemental Figure 2

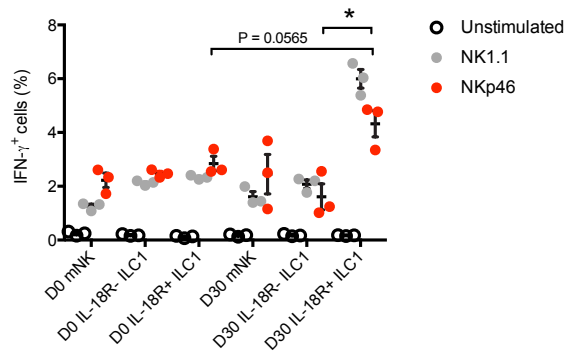


Supplementary Figure 2

Figure S2. Related to Figure 3. Memory T cell populations increase the expression of cytokine receptors following the resolution of infection.

(a,b) Graph shows average mRNA expression of indicated cytokine receptors in splenic OT-I CD8⁺ T Cell sorted from **(a)** Listeria-OVA and **(b)** VSV-OVA infected mice at indicated time-points PI, as assessed by microarray (Data provided by Immunological Genome Consortium⁵⁴). **(c-d)** Graph shows mRNA expression of indicated cytokine receptors by **(c)** naïve and LCMV experienced primary and secondary memory GP66-CD4⁺ T cells post LCMV infection and by **(d)** resting and inflammation experienced memory Tregs, assed by RNA-sequencing as was previously reported²³. Data are representative of 2 independent experiments with **(c)** n=3 and **(d)** n=5 mice per group. Data are presented as the mean ± SEM.

Supplemental Figure 3



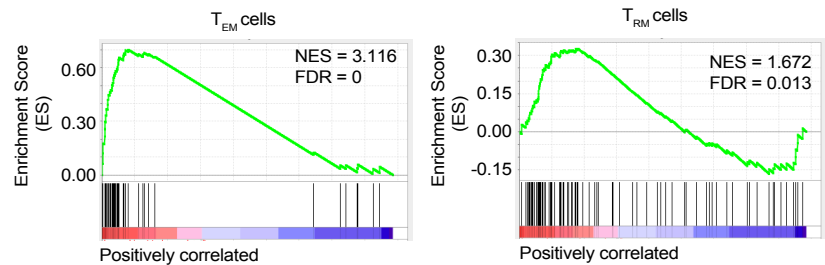
Supplementary Figure 3

Figure S3. Related to Figure 4. IL-18 α^+ ILC1 display enhanced IFN- γ production following stimulation of activating receptors.

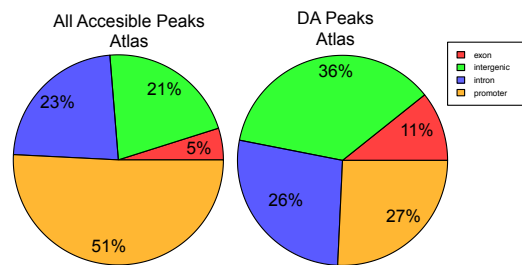
WT mice were infected with MCMV (i.p.) and liver was harvested and analyzed 30 days PI. Graph shows percentage of IFN- γ^+ cells within indicated liver ILC1 populations following plate-bound stimulation with either media alone, α NKp46, or α NK1.1 plate-bound antibodies compared to uninfected mice. Data are representative of 3 independent experiments with n=3 mice per group. Samples were compared using a two-tailed Student's t test, and data are presented as the mean \pm SEM (*p<0.05).

Supplementary Figure 4

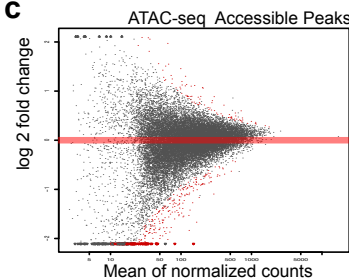
a



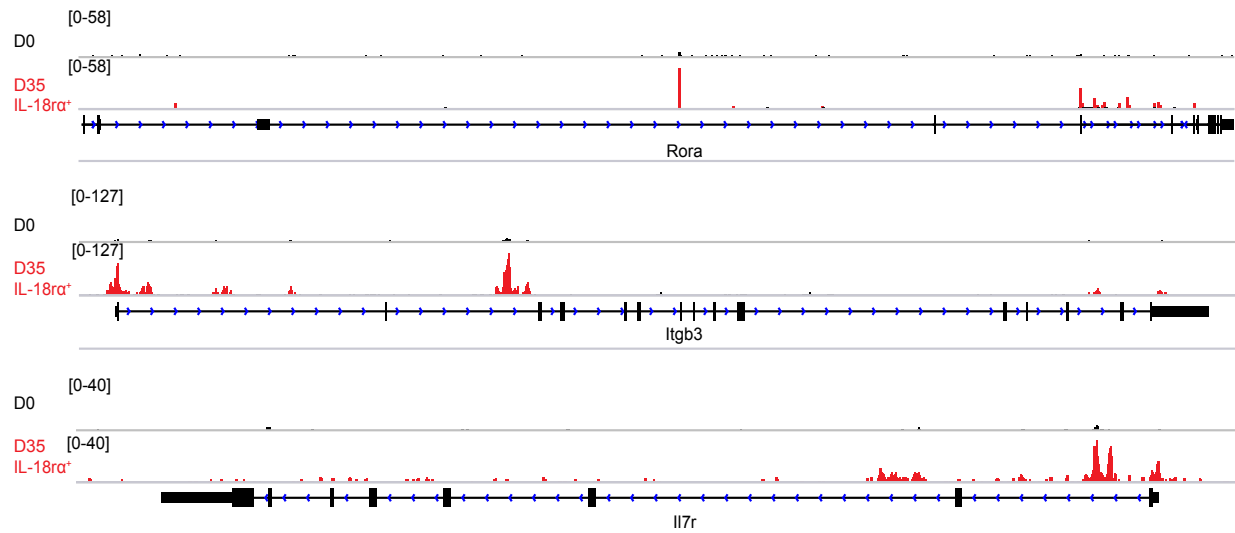
b



c



d

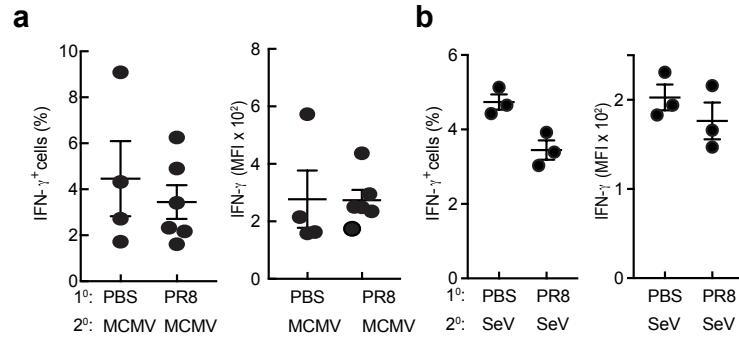


Supplementary Figure 4

Figure S4. Related to Figure S5. Memory ILC1 have distinct transcriptome and epigenomes compared to naïve ILC1.

(a) Gene set enrichment analysis (GSEA) of genes upregulated in D35 IL-18 α^+ ILC1 over D0 ILC1 from genes upregulated in effector memory T cells (T_{EM}) (left) or resident memory T cells (T_{RM}) (right) compared to naïve T cells after LCMV infection, assessed by RNA-sequencing as was previously reported³². (NES, normalized enrichment score; FDR, false discovery rate; NES, normalized enrichment score assessed by an empirical phenotype based permutation test assuming a null distribution). **(b)** Absolute numbers and proportion of all peaks (23016 total) and differentially accessible (DA) peaks in peak atlas (373 total, p value less than 0.2). **(c)** MA plots of differentially accessible regions (red dots) of all peak types comparing D0 vs D35 IL-18 α^+ ILC1. **(d)** Representative ATAC-sequencing tracks show accessible regions for *Rora*, *Itgb3*, and *Ii7r* in naïve and memory ILC1. Y axis depicts normalized counts, while x axis displays genomic axis with scale bar. Data are representative of 2 replicate experiments with n=2 samples of n=20 mice per condition. All adjusted p values were indeed determined using DESeq2 and were two-sided.

Supplemental Figure 5



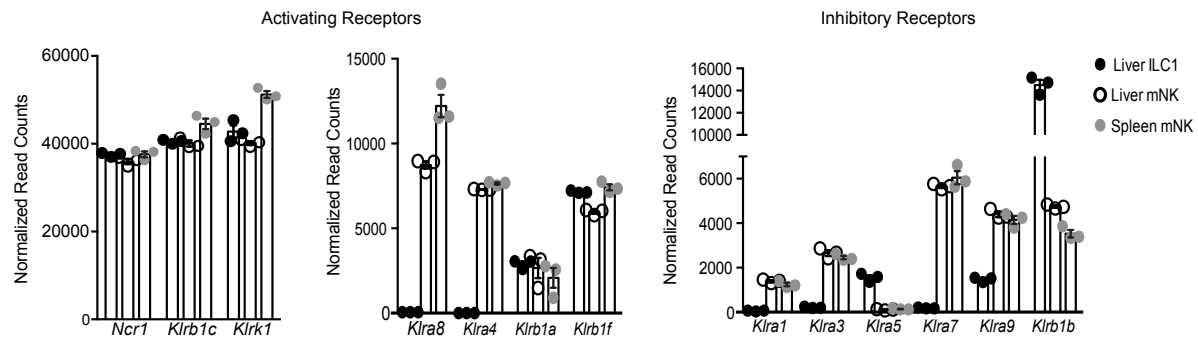
Supplementary Figure 5

Figure S5. Related to Figure 6. Induction of ILC1 memory is MCMV specific and cannot be formed by other viruses.

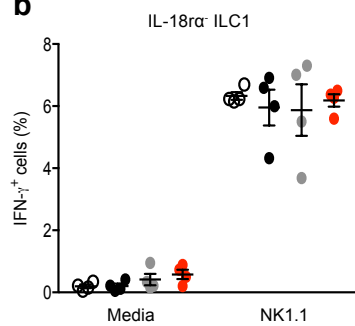
WT mice were injected initially with either PBS or Influenza-PR8 intranasally (i.n.). 28 days PI, mice were subsequently challenged with either MCMV (i.n.) or Sendai virus (Sev) and analyzed 48 hours PI. **(a)** Quantification of intracellular IFN- γ staining by percentage and MFI of ILC1 at 48 hours following primary and secondary MCMV challenge in i.v. CD45 unlabeled fraction of the lung. **(b)** Quantification of intracellular IFN- γ staining by percentage and MFI of ILC1 at 48 hours following primary and secondary SeV challenge in i.v. CD45 unlabeled fraction of the lung. Data are representative of 3 independent experiments with **(a)** $n=4$ mice and **(b)** $n=3$ per group. Data are presented as the mean \pm SEM.

Supplemental Figure 6

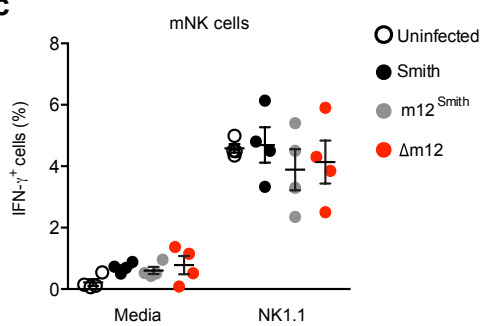
a



b



c



Supplementary Figure 6

Figure S6. Related to Figure 6. The MCMV-encoded protein m12 does not drive memory formation of IL-18 α ⁻ ILC1.

(a) Graph shows mRNA expression of indicated Group 1 ILC specific activating and inhibitory receptors in resting liver ILC1, liver mNK, and splenic mNK, obtained by RNA-sequencing as was previously reported¹². (b-c) WT mice were infected with indicated MCMV strains i.p. and liver ILC1 were analyzed 30 days PI. Quantification of IFN- γ ⁺ cells within liver for (b) IL18 α ⁻ ILC1 and (c) mNK following plate-bound stimulation with either media alone or α NK1.1 antibody. Data are representative of 3 independent experiments with (a) n=3 mice and (b) n=4 per group. Data are presented as the mean \pm SEM.